

Synergistic Interface Engineering in ZnO@CNT Catalysts:
Electronic Modulation for Switching Peroxydisulfate Activation
toward a $^1\text{O}_2$ -Dominated Non-Radical Pathway

1 **S1. Experimental materials**

2 Zinc nitrate hexahydrate ($\text{Zn}(\text{NO}_3)_2 \cdot 6\text{H}_2\text{O}$; AR,99%), multi-walled carbon
3 nanotubes (CNTs), 2-methylimidazole (2-MI; AR,99%), 2,2,6,6-
4 tetramethylpiperidine (TEMP; AR,99%), methanol (MA; AR,99%),
5 potassium persulfate (PDS; $\text{K}_2\text{S}_2\text{O}_8$), sulfamethoxazole (SMX; AR,99%), p-
6 Benzoquinone (p-BQ; AR,99%), L-histidine(L-His; 99%), tert-butanol (TBA;
7 AR,99%), sodium bicarbonate (NaHCO_3 ; AR,99%), sodium perchlorate,
8 sodium nitrate (NaNO_3 ; AR,99%), humic acid (HA; AR,99%), and sodium
9 hydroxide (NaOH; AR,96%). Methanol (chromatographically pure),
10 ciprofloxacin (CIP; AR, 99%), diclofenac (DF; AR, 99%), bisphenol A (BPA;
11 AR, 99%). All chemicals were purchased from Shanghai Macklin
12 Biochemical Technology Co., Ltd. All reagents were of analytical grade and
13 used without further purification.

14 **S2. Characterizations**

15 Scanning electron microscopy (SEM) and energy spectrum analysis (EDX)
16 systems were used to characterize the surface morphology and elemental
17 distribution of the ZnO@CNT composites, and X-ray diffractometry (XRD,

18 Cu K α radiation source, $\lambda = 1.5406 \text{ \AA}$) was used for physical structure
19 analysis. Electrochemical impedance spectroscopy (EIS, CHI1650E) was
20 used to electrochemically analyze the samples. The degradation of various
21 contaminants was tested by HPLC (Agilent Technologies 1260 Infinity II).
22 Condition: column: Hypersil ODS C18 150*4.6mm; T=35 °C; u = 1.0 ml/min.
23 We used spin trapping (DMPO, TEMP) techniques to detect $\text{SO}_4^{\cdot-}$, $\cdot\text{OH}$, $\text{O}_2^{\cdot-}$,
24 and $^1\text{O}_2$ radicals, and electron paramagnetic resonance (EPR) was used to
25 detect DMPO- $\text{SO}_4^{\cdot-}$, DMPO- $\cdot\text{OH}$, DMPO- $\text{O}_2^{\cdot-}$, and TEMP- $^1\text{O}_2$ signals.
26 Different samples were prepared in order to capture $\text{SO}_4^{\cdot-}$, $\cdot\text{OH}$, $\text{O}_2^{\cdot-}$, and $^1\text{O}_2$
27 radicals. For example, the $\cdot\text{OH}$ and $\text{SO}_4^{\cdot-}$ samples were prepared from 50 μL
28 of DMPO, 0.5 mL of deionized water and 0.5 mL of reaction solution, while
29 the $^1\text{O}_2$ sample was prepared from 50 μL of TEMP and 0.5 mL of reaction
30 solution. The samples were then sent to a BRUKER A300 spectrometer for
31 analysis, with the test conditions set to a modulation amplitude of 1.0 G, a
32 time constant of 10.24 ms, a transition time of 81.92 ms, and a scan time of
33 83.89 s. We used Win-EPR and SimFonia version.

34 **S3. Software for data processing and analysis**

35 The degradation kinetics were fit by the pseudo first-order model and the
36 apparent rate constant (k) was calculated according to Eq. (B1):

$$37 \quad \ln (C_t / C_0) = -k t \quad (\text{B1})$$

38 where C_t is the target pollutant concentration at a certain reaction time (t), and
39 C_0 is the initial concentration of target pollutant.

40

41 **S4. Theoretical calculations**

42 The DFT calculations were conducted by employing the universal generalized
43 gradient correlation function and Vienna ab initio simulation package
44 (VASP5.4). A plane-wave basis set with cutoff energy at 400 eV within the
45 framework of the projector augmented wave method was adopted. The
46 Gaussian smearing width was set to 0.2 eV. The Brillouin zone was sampled
47 with $3 \times 3 \times 1$ K points. All atoms were allowed to converge to 0.01 eV Å⁻¹.

48 The condensed Fukui function could be calculated as:

49 Nucleophilic attack: $f_k^+ = q_N^k - q_{N+1}^k$ (B2)

50 Electrophilic attack: $f_k^- = q_{N-1}^k - q_N^k$ (B3)

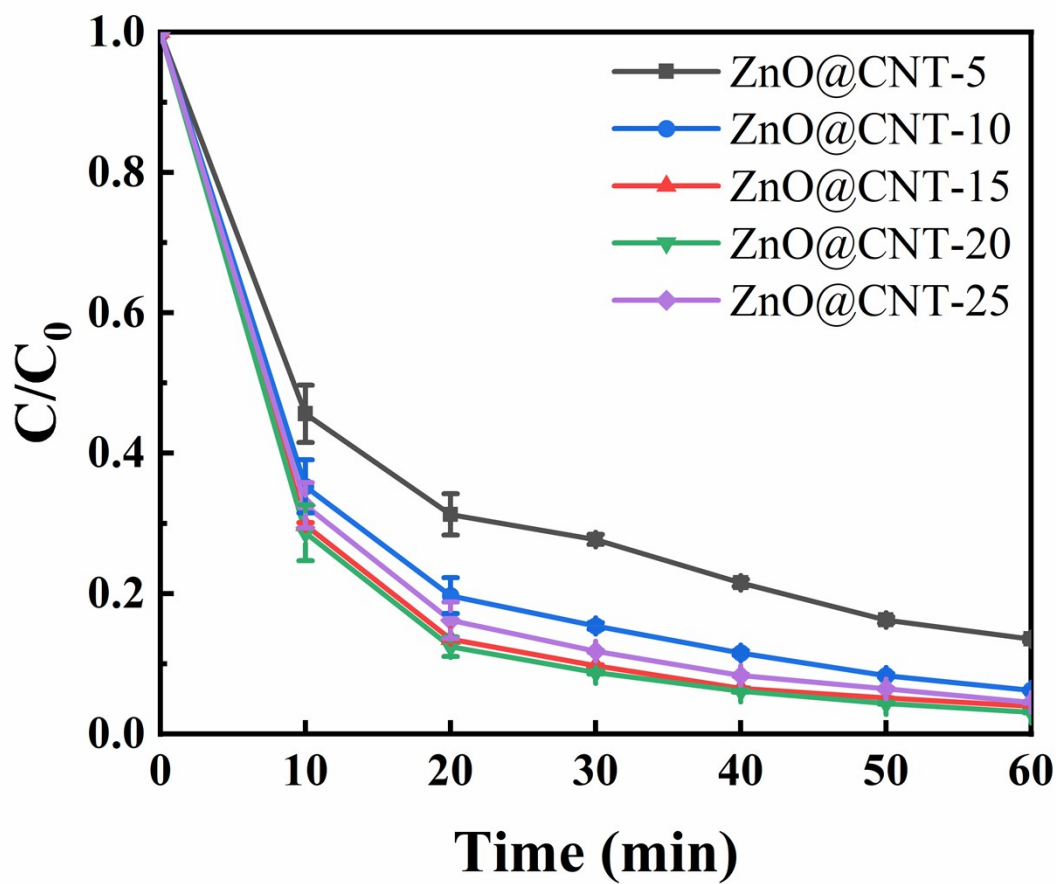
51 Radical attack: $f_k^0 = (q_{N-1}^k - q_{N+1}^k)/2$ (B4)

52 Where q_k was the atom charge of atom K at corresponding state, and the
53 values of Fukui Index of the reactive sites were usually larger than other
54 regions.

55 **S5. Degradation efficiency of SMX by ZnO@CNT with different loadings**

56 As shown in the degradation trends, SMX removal efficiency increased
57 with ZnO loading from 5% to 20%, but a decline was observed at 25%

58 loading. Specifically, at 30 minutes of reaction time, the degradation
59 efficiencies of ZnO@CNT-5, 10, 15, 20, and 25 were 72.3%, 84.6%, 90.3%,
60 91.2%, and 88.2%, respectively. This trend indicates that 15-20% loading
61 represents the optimal range, with 15% loading showing near-peak
62 performance. More importantly, when evaluating ZnO utilization efficiency,
63 the incremental improvement from 15% to 20% loading was minimal (only
64 0.9% increase in efficiency), while the 25% loading showed decreased
65 performance due to particle aggregation and reduced active site accessibility,
66 as confirmed by our characterization studies. From an economic perspective,
67 ZnO@CNT-15 achieves comparable performance to ZnO@CNT-20 while
68 using 25% less ZnO precursor, representing a more cost-effective
69 formulation. Additionally, moderate loading of 15% provides better long-term
70 stability prospects, as excessive metal oxide loading can accelerate catalyst
71 deactivation due to particle aggregation and potential mass transfer
72 limitations. Therefore, considering the balance between catalytic
73 performance, material utilization efficiency, and practical applicability,
74 ZnO@CNT-15 was selected as the optimal catalyst for detailed mechanistic
75 studies in this work.

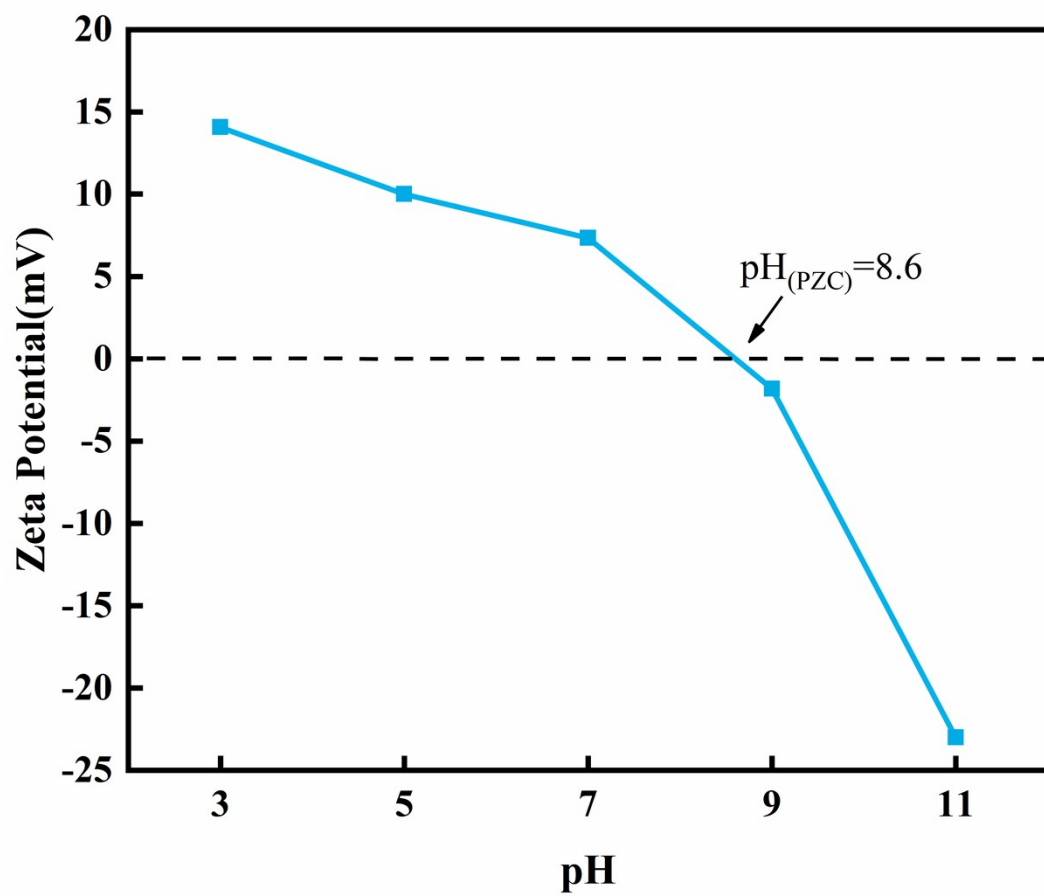


76

77 Fig. S5. Degradation efficiency of SMX by ZnO@CNT with different

78

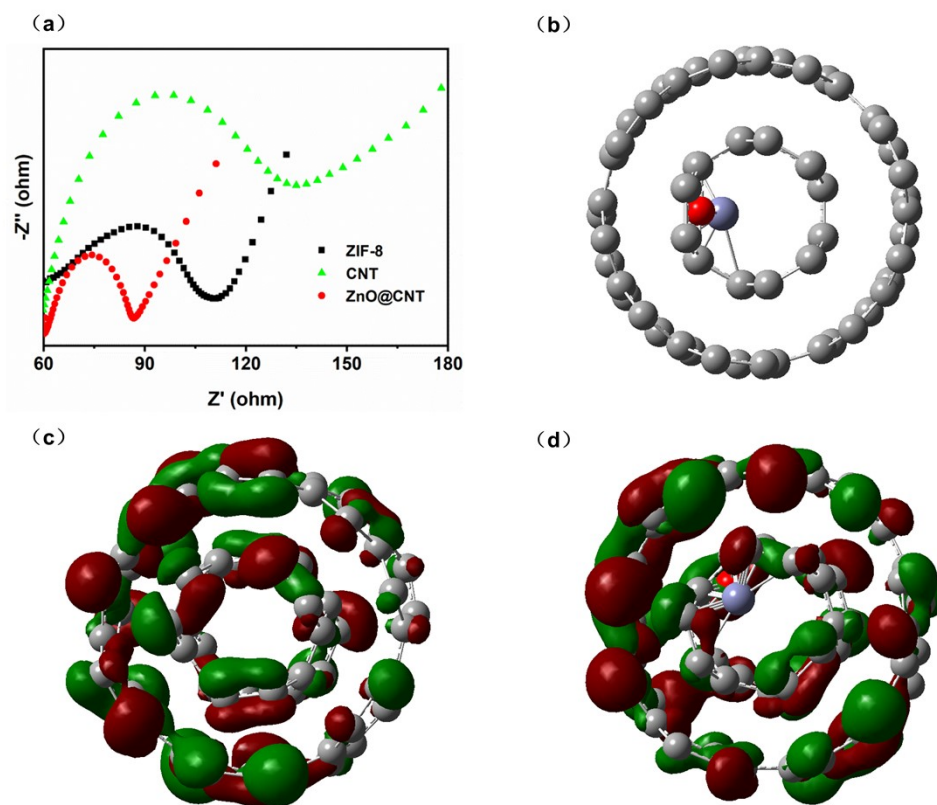
loadings



79

80

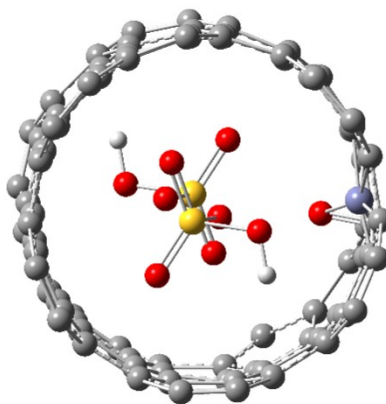
Fig. S6. Zeta potential of ZnO@CNT at different pH conditions.



81

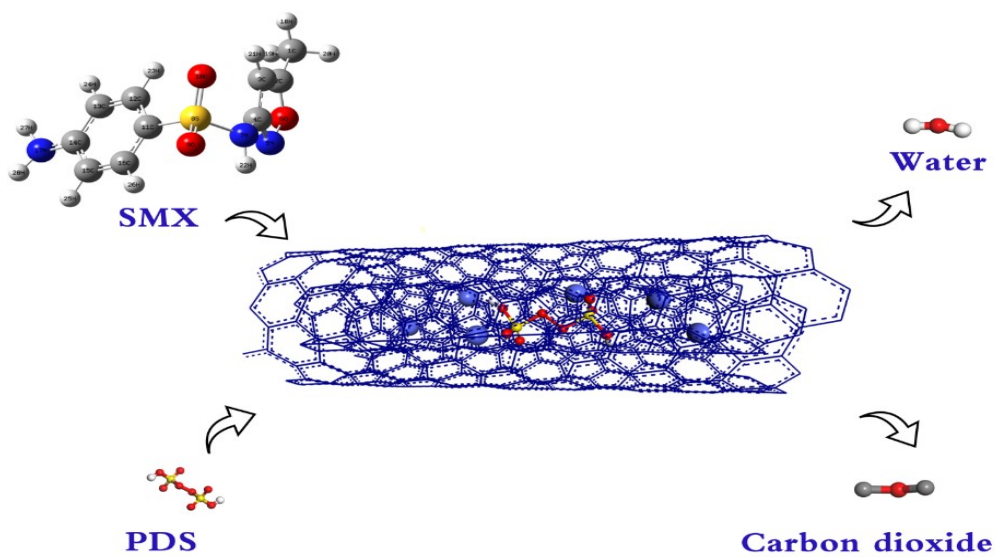
82 Fig. S7. EIS of ZIF-8, CNT and ZnO@CNT (a); ZnO@CNT Load model (b);

83 Carbon nanotube HOMO diagram (c); ZnO@CNT HOMO diagram (d).



84

85 Fig. S8. Potential adsorption models of PDS molecules on ZnO@CNT.



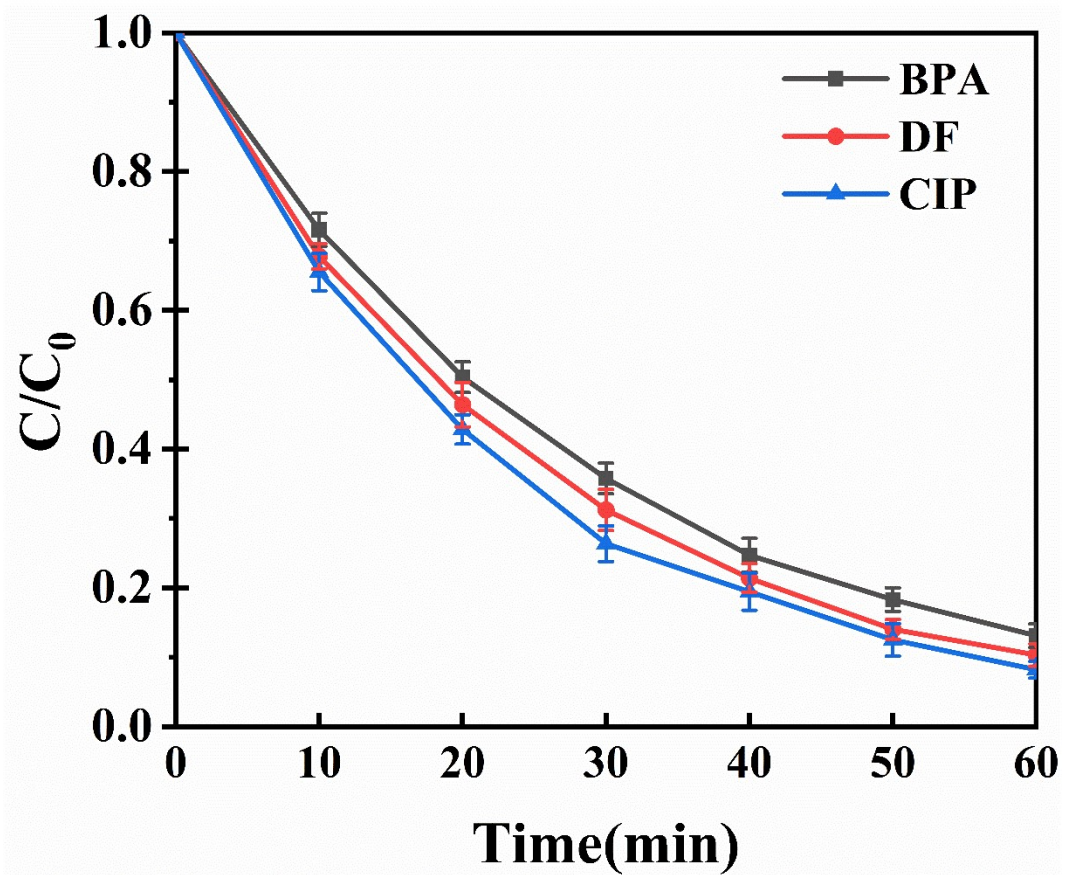
86

87 Fig. S9. Degradation mechanism of SMX in ZnO@CNT/PDS system.

88

89

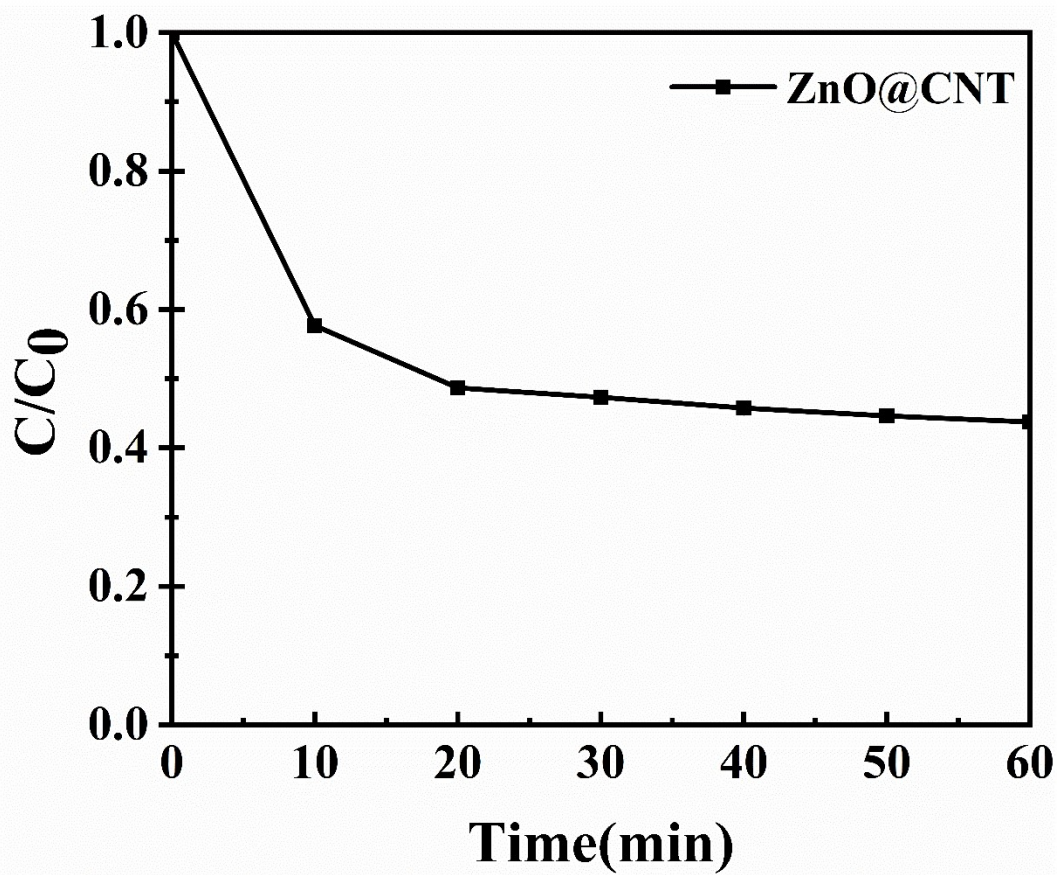
90



91

92 Fig. S10. Degradation performance of ZnO@CNT for CIP, DF and BPA

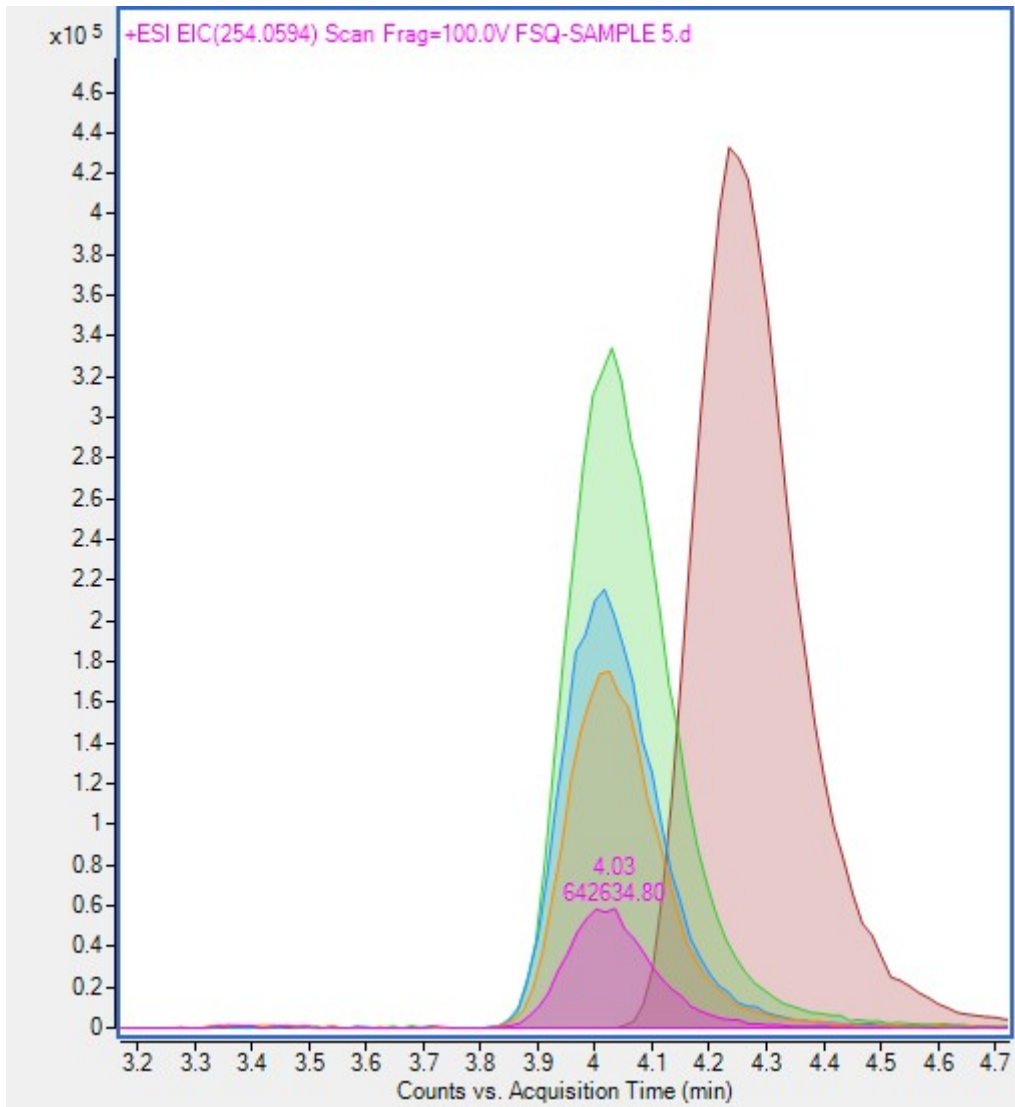
93



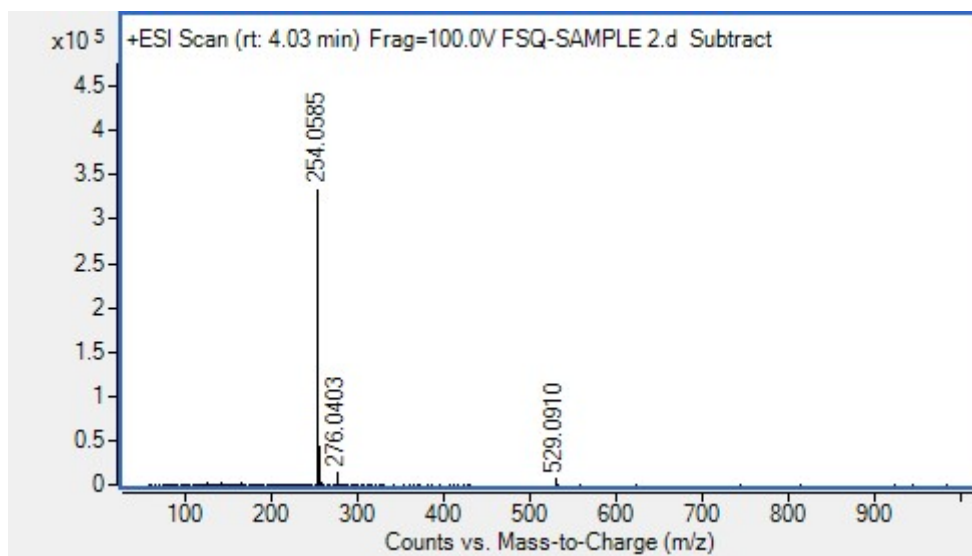
94

95 Fig. S11. The TOC of ZnO@CNT/PDS [PDS] = 0.8 g/L, SMX = 20 mg/L,

96 [ZnO@CNT] = 0.2 g/L, [pH] = 9, Temperature = 25 °C.



97



98

99 Fig. S12. LC-MS chromatograms of SMX and the transition products

100